ACS APPLIED ENERGY MATERIALS

www.acsaem.org Letter

Highly Durable Platinum Catalysts on Nano-SiC Supports with an Epitaxial Graphene Nanosheet Layer Grown from Coffee Grounds for Proton Exchange Membrane Fuel Cells

Byeong Geun Kim,[‖] Seokhee Lee,[‖] Yi kyeong Jung, Jin Uk Lee, Seoyoon Shin, Tae Ho Shin,* and Soon-Mok Choi*

Cite This: *ACS Appl. Energy Mater.* 2023, 6, 4103−4110 Read Online

ACCESS | Metrics & More | Article Recommendations | Supporting Information

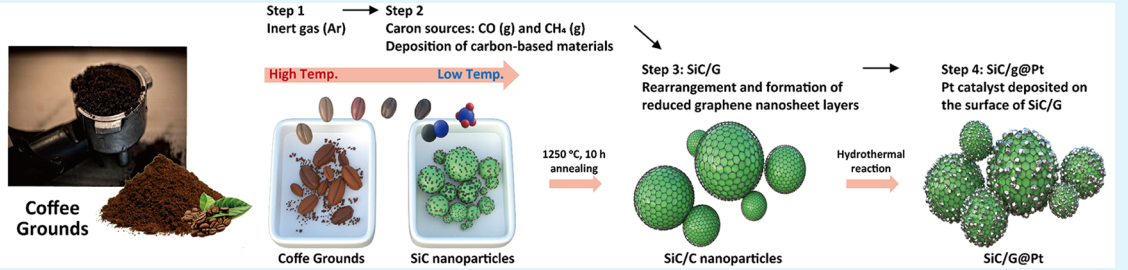

ABSTRACT: Robust ceramic supports have attracted significant attention as alternatives to carbon supports for proton exchange membrane fuel cells (PEMFCs). However, they suffer from lower electrocatalytic activities than carbon-based supports because of their electrical conductivity. Here, SiC nanopowders were modified with epitaxial graphene and evaluated as the support for Pt in PEMFCs. Coffee grounds are used as a carbon source to not only enhance the electrocatalytic activity of the graphene-modified SiC supports but also demonstrate the feasibility of exploiting and commercializing this widely available waste product. The Pt-decorated ceramic supports deliver the enhanced durability and performance under the accelerated electro′chemical conditions.

KEYWORDS: *proton exchange membrane fuel cells (PEMFCs), ceramic support, SiC, graphene nanosheet, oxygen reduction reaction (ORR)*

1. INTRODUCTION

The hydrogen energy sector has received a great deal of attention because of its potential to provide environmentally friendly power storage and generation with no pollution and to realize carbon neutrality. To achieve this more recent aim of carbon neutrality, the power trains of various vehicles that rely on fossil fuels should mostly be changed to electric power trains operating on green energy devices, including hydrogen fuel cells such as proton exchange membrane fuel cells (PEMFCs) to decrease carbon emissions on the road. Although several PEMFCs have been successfully launched on the green mobility market, the operation of heavy vehicles powered by fuel cells imposes severe durability and performance constraints on the electrocatalyst, beyond the demand for the decreasing Pt group metal (PGM) loading contents in the interest of cost-effectiveness.[1] In particular, a long lifetime and high power density are even more critical for the potential application of PEMFCs in heavy-duty trucks than they are in purely electric vehicles.[2]

Currently, carbon-supported platinum (Pt/C) materials, which are composed of Pt nanoparticles stably dispersed on conductive carbon black as both a support and a source of a large amount of active sites, are widely employed as cathode catalysts owing to their appropriate activity toward the oxygen reduction reaction (ORR).[3] However, the lifetime of the electrocatalyst must meet the requirements of steady operation for 8000 h for its practical employment in the expanded PEMFC market.[4] The ORR activity highly depends on the size and dispersion of Pt catalysts on the carbon support as well as the interactions between these two components. During practical electrochemical operation conditions such as current load cycling, high current, and start-up/shut-down, the electrocatalyst mainly decays because of Pt particle coarsening and the Pt catalyst detaching from the support.[5−8] The degradation mechanisms of PEMFC catalysts that have typically been investigated in detail thus far include (1) Pt dissolution, (2) Ostwald ripening, (3) agglomeration, (4) particle detachment, and (5) carbon corrosion. These

Received: December 19, 2022
Accepted: April 5, 2023
Published: April 14, 2023

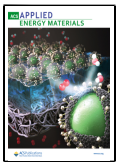

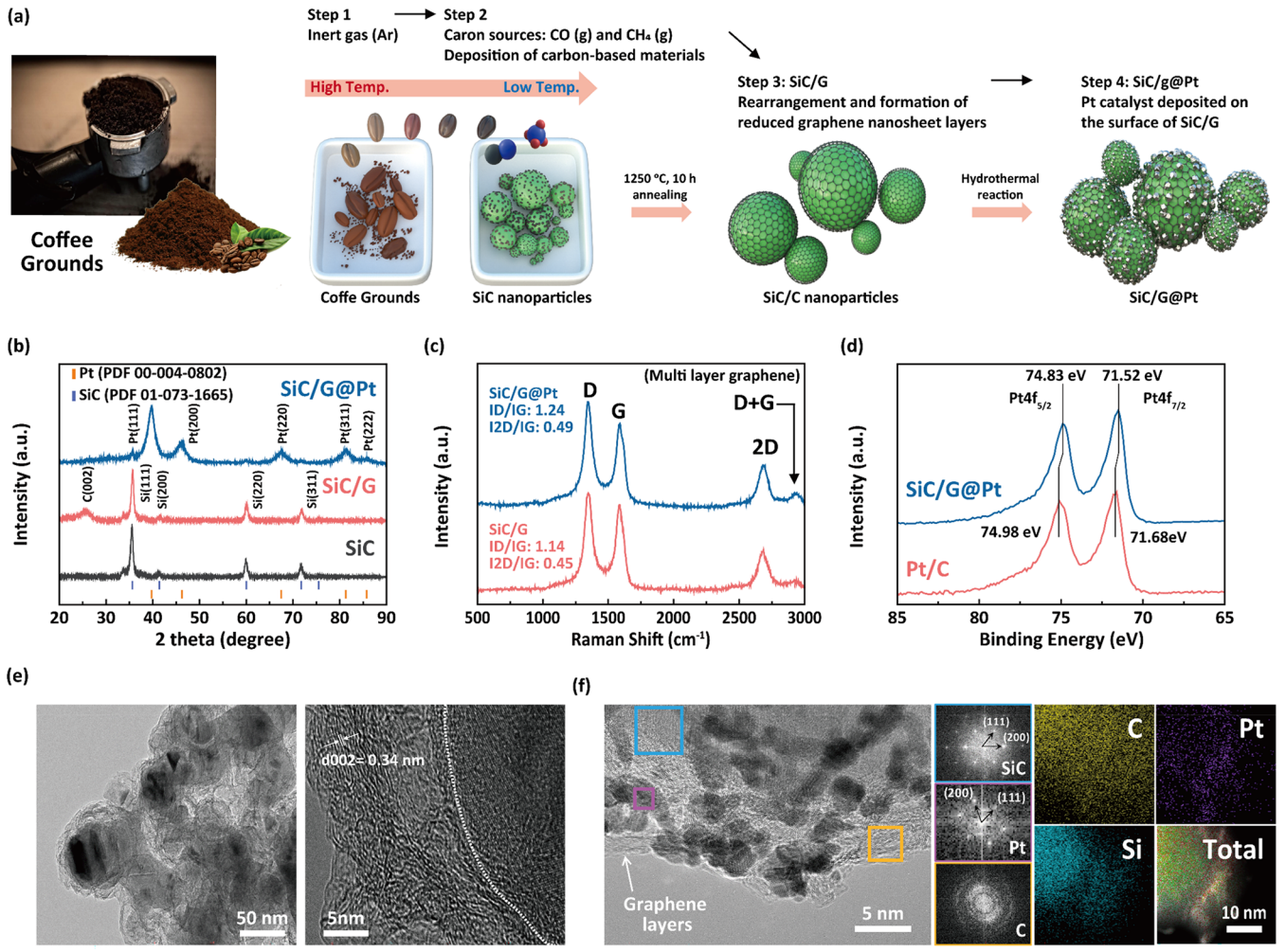

Figure 1. (a) Schematic of the process for synthesizing SiC/G@Pt catalysts. Carbon-based sources such as CH_4(g) and CO(g) are vaporized from coffee grounds in the presence of SiC nanopowder (step 1), and then, C(s) atoms are deposited on the SiC nanoparticle surfaces (step 2). Functionalized graphene layers form on the SiC after rearranging and crystallizing at a relatively low temperature (step 3). Finally, Pt nanoparticles are deposited on the surface of SiC/G (step 4). (b) XRD patterns of materials: SiC nanopowder, synthesized SiC/G, and SiC/G@Pt. (c) Raman spectra of the synthesized SiC/G and SiC/G@Pt samples. (d) High-resolution XPS analysis of Pt 4f peaks from SiC/G@Pt and commercial Pt/C (d) TEM images of SiC/G. (e) TEM image of SiC/G@Pt and fast Fourier transform (FFT) diffraction patterns of SiC, C, and Pt with EDS elemental mapping of SiC/G@Pt.

mechanisms always exhibit a complex interplay as the Pt electrocatalytic activity electrochemically accelerates carbon corrosion in acidic aqueous conditions. Subsequently, the oxidation of carbons hinders interactions between the Pt catalyst and support, thus causing Pt to detach and agglomerate.[9] Therefore, not only improving ORR activity but also preventing the corrosion of carbon in the cathode catalysts should be addressed as key technical challenges in improving their durability. To that end, alternative support materials must be explored, such as nanostructured graphite, carbon nanotubes (CNTs), graphene, and noncarbon materials to build robust, durable composite electrocatalysts with high catalytic activities.

Several advanced nanostructured carbons with high crystallinity, including CNTs, carbon fiber, and reduced graphene oxide (rGO), are more resistant to carbon corrosion than the conventional carbon black support. Unfortunately, however, these carbon-based materials remain vulnerable to corrosion and carbon oxidation. Therefore, noncarbon supports such as inorganic oxides and carbides have recently been attracting attention as they can completely avoid electrochemical carbon corrosion, in contrast with carbon materials. Among numerous inorganic oxide support materials, several groups have used TiO_2-based supports to stabilize the Pt catalyst and provide strong metal support interactions, which has resulted in smaller losses in the ORR activity compared with that of commercial Pt/C.[9−11] However, most oxide supports suffer from electrical insulating properties and a low surface area. Therefore, blending them with CNTs and doping with them n-type additives have been investigated to impart oxide supports with electrical conductivity. For example, Behm et al. proposed nanostructured TiO_2 on CNTs (TiO_2@CNT) as a support.[12] Furthermore, Yoo et al. recently used a N,C codoped TiO_2 support to achieve high ORR activity and dramatically enhanced durability with only a 7% loss in the electrochemical surface area (ECSA) after 10,000 cycles.[13] Meanwhile, carbide-based materials have rarely been studied as alternative catalyst supports for PEMFCs, although they have relatively higher electrical conductivity and stability in acidic and oxidative environments than oxide materials. In particular, SiC is widely used as a structural ceramic and can be an electrical conductor or a

https://doi.org/10.1021/acsaem.2c04073
ACS Appl. Energy Mater. 2023, 6, 4103−4110

semiconductor with a fairly large band gap, depending on the lattice structure and the type of doping. The good chemical and mechanical properties of SiC have the potential to perfectly meet the requirements of a robust support for PEMFCs. However, SiC is not a proton conductor and has a lower electrochemical surface activity than conventional carbon supports.

To overcome these shortcomings of SiC, this study successfully grew graphene layers on SiC nanoparticles to improve their surface electrocatalytic activity and to promote interactions between the Pt catalyst and the SiC-based support. Specifically, we used discarded coffee grounds as the carbon source to cover the SiC surface with an epitaxial graphene nanosheet. We also proposed two possible carbon deposition sources: (i) gases from the thermally decomposed coffee waste and (ii) the thermal decomposition of surface layers of SiC because of the high processing temperature (above 1000 °C), both of which are practical strategies for preparing an alternative catalyst support for PEMFCs. Then, the Pt catalysts supported by nanographene-modified SiC (SiC/G@Pt) were used to prepare a PEMFC cathode for the first time, and their fuel cell performance and durability were characterized. Our study aimed to demonstrate that the synthesized SiC@G support exhibits enhanced ORR activity and fuel cell performance as well as ultrahigh stability during 5000 cycles.

2. RESULTS AND DISCUSSION

Our strategy for growing epitaxial graphene nanolayers on the surface of SiC using coffee grounds is schematically illustrated in Figure 1a. Coffee grounds are known to be composed of cellulose, hemicellulose, lignin, etc.[14] These components thermally decompose into various byproducts such as CO_2(g), CO(g), and CH_4(g).[15] Li et al. observed that carbon oxides (CO_2 and CO) and hydrocarbons (CH_4, C_2H_4, and C_6H_6) were produced from spent coffee grounds.[15] They confirmed that CO(g) and CH_4(g) were the primary volatile gases generated during pyrolysis at 1000 °C with a low heating rate. CO(g) and/or CH_4(g) have been used to synthesize carbon nanostructures such as CNTs[16−18] and graphene.[19] Two different general mechanisms have been reported for forming graphene layers on SiC: (1) directly coating graphene layers from carbon sources such as CH_4, CO, and CO_2 using chemical vapor deposition (CVD) processes[19,20] and (2) forming graphene layers by thermally decomposing SiC on its surface.[21] In our research, CO(g) and CH_4(g) are proposed as carbon sources for the formation of graphene layers on SiC nanopowder. When these gases adsorb on the surface of SiC/G nanopowder, they may change into solid carbon through the following reactions:

$$CH_4(g) \rightarrow C(s) + 2H_2(g) \quad (1)$$

$$CO(g) \rightarrow C(s) + O(g) \quad (2)$$

We hypothesized the following formation mechanism: When carbon-based materials such as CH_4(g) and CO(g) vaporize from coffee grounds to SiC nanopowder, C(s) atoms deposit on the surface of SiC nanopowder (steps I and II in Figure 1a). After they rearrange and crystallize at a relatively low temperature, a few epitaxial graphene layer form on the surface of SiC nanopowder (SiC/G, step III in Figure 1a). In addition, the thermal decomposition of SiC may have contributed to the formation of graphene layers on the SiC nanoparticles because the processing temperature was sufficiently high (above 1000 °C).[22,23] Specifically, after Si(s) atoms vaporize, residual C(s) atoms may be used as carbon sources for graphene layers, in addition to carbon from external sources. Finally, Pt nanoparticles are deposited on the surface of the SiC/G during the hydrothermal method (step IV in Figure 1a). The typical values of the composition analysis of the catalysts are shown in Table S1. The electrical conductivities of powder samples under air are plotted as a function of the pressure as shown Figure S3. The apparent electrical conductivity of Pt/C and SiC/G@Pt are only 2.54 and 2.56 S cm^{-1}, respectively. The apparent electrical conductivities of Pt-supported catalysts and SiC/C are significantly enhanced compared to that of SiC alone. Therefore, the electrical conductivity of SiC nanoparticles tends to be influenced in general by the apparent electrical conductivities of the reduced graphene oxide and Pt nanoparticles.

As evidenced by the X-ray diffraction (XRD) pattern in Figure 1b, we successfully synthesized SiC/G using carbon from the thermal decomposition of coffee grounds (Figure 1b). Notably, peaks corresponding to SiC(111), (200), (220), and (311) are clearly observed at 2θ = 35.5°, 59.9 °, and 71.7 ° (ICDD: 00-029-1131) as well as peak of reduced graphene oxide after the formation of carbon layer on the surface of SiC is shown at 2θ = 26.7°. Pt characteristic peaks appeared at at 2θ = 39.6°, 47.1 °, 67.4 °, 82.2 °, and 86.4 °, corresponding to the diffraction from Pt(111), Pt(200), Pt(220), Pt(311), and Pt(222). The Pt peaks are assigned according to the International Centre for Diffraction Data PDF 00-004-0802 and show a face-centered-cubic crystal structure for platinum.

The growth of epitaxial graphene on the SiC surface was also confirmed by Raman spectroscopy (Figure 1c). To identify the structure of graphene materials that significantly interact with the SiC surface, the ratio of the D and G band intensities (I_D/I_G) was calculated, which are the disorder and graphitic bands, respectively. The Raman spectrum of SiC/G and SiC/G@Pt shows D and G peaks at ∼1350 and ∼1595 cm^{-1}, respectively, thus confirming lattice distortion.[24,25] The resulting I_D/I_G ratio of SiC/G@Pt and SiC/C is approximately 1.24 and 1.14, respectively. These results can be considered large, which may be attributed to the decreased sp^2 cluster size in the defective graphene structure that formed during epitaxial growth in the oxygen-poor chemical vapor atmosphere generated by the coffee grounds.[26] Accordingly, the I_D/I_G ratio of ca. 1.07 agrees with a previously reported I_D/I_G ratio for rGO that was larger than 1.0.[27] The G band is attributed to the first-order scattering of the E_{2g} phonon of the sp^2 C−C bond, whereas the D band represents the defective functionalization associated with vacancy-type defects.[28] Interestingly, the superior electrocatalytic activity discussed below may be understood in terms of the similarity between the functionalized graphene layer on the SiC surface and rGO because one of the most critical differences between graphene materials and rGO is their electrical conductivities.

To confirm the effect of SiC/C for electrocatalytic system, the high-resolution XPS analysis of Pt 4f peaks from SiC/G@Pt and commercial Pt/C as shown in Figure 1d. A shift of the Pt 4f binding energy of SiC/G@Pt toward lower energies compared with the corresponding commercial Pt/C catalyst indicated that there is a strong metal−support interaction (SMSI) between Pt nanoparticles and SiC/C.[29−31] Further, deconvolution of the Pt 4f peak from SiC/G@Pt indicates that the platinum surface with metallic form is increased in

https://doi.org/10.1021/acsaem.2c04073
ACS Appl. Energy Mater. 2023, 6, 4103−4110

Table 1. ECSA and ORR Performance of Catalysts before and after 5000 Cycles under ADT Conditions in 0.1 M $HClO_4$

samples	ECSA (m^2/g_{pt})	onset potential (V)	half potential (V)	MA (mA/mg_{pt}) @ 0.9 V_{RHE}	SA (mA/cm^2) @ 0.9 V_{RHE}	limit current (mA/cm^2)	ECSA loss (%) @ 1.0−1.5 V
SiC/G@Pt initial	44.36	0.90	0.79	9.92	0.024	−5.02	26.89
SiC/G@Pt 5k cycles	32.43	0.90	0.77	8.34	0.026	−5.01	
Pt/C initial	47.62	0.91	0.82	11.20	0.024	−5.35	36.88
Pt/C 5k cycles	30.06	0.83	0.68	0.36	0.002	−4.89	

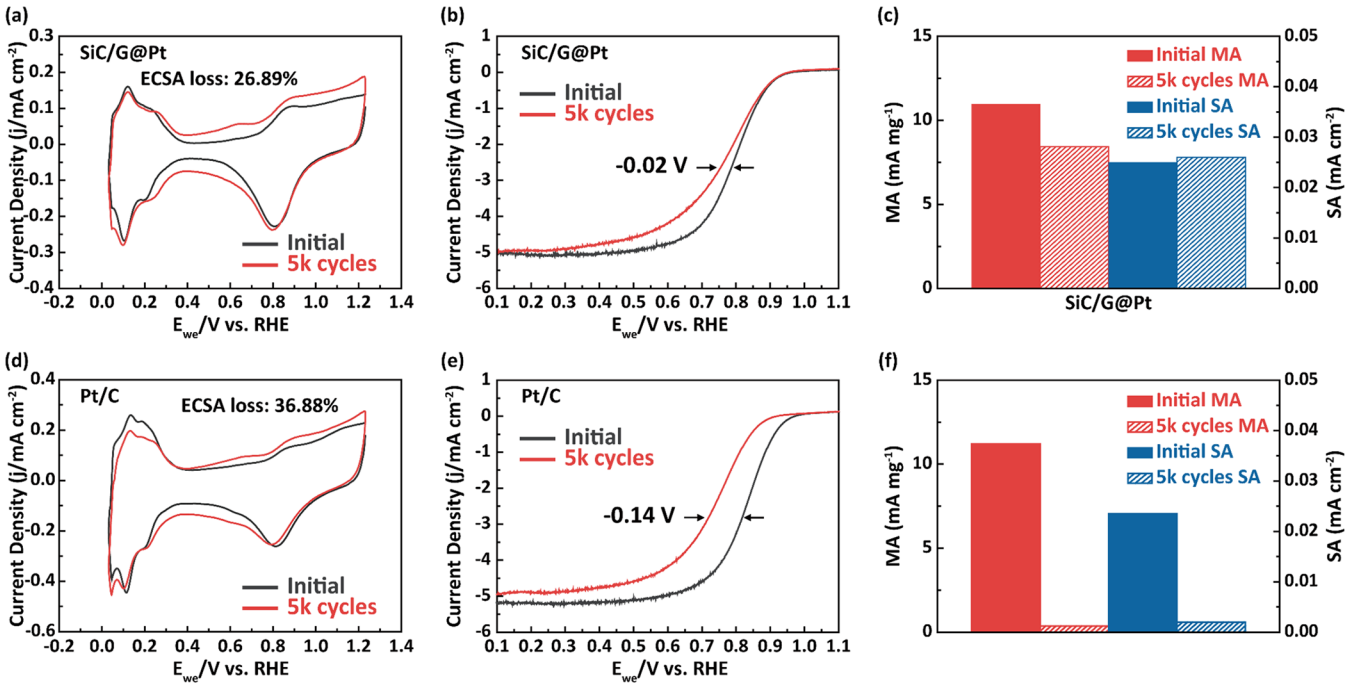

Figure 2. Electrochemical analysis of SiC/G@Pt (top) and Pt/C catalysts (bottom) before and after ADT for 5000 cycles in 0.1 M $HClO_4$: (a, d) CV curves; (b, e) ORR polarization curves; and (c, f) mass activity (red) and specific activity (blue) at 0.9 V.

comparison of that of Pt/C (Figure S2 and Table S3). This kind of "metal-support interaction" can modify the electronic and catalytic properties of metal nanoparticles and leads to the activation of the dispersed metal catalysts.

The epitaxial graphene was observed using transmission electron microscopy (TEM), which confirmed that it was deposited on the entire surface of the SiC nanoparticles (Figure 1e) to a thickness of ∼5−7 nm. After Pt was deposited on the SiC/G surface, Pt catalysts appeared to be well distributed with diameters of approximately 3−5 nm. Moreover, the fast Fourier transform (FFT) diffraction patterns of SiC and Pt in Figure 1f indicate the crystal orientations of SiC and Pt, confirming the XRD results. The epitaxial graphene formed on the surface of SiC presents 2 θ= 26.7 degree corresponding to *d*-spacing of 0.34 nm, which might be attributed to rGO layers (see *d*-spacing of the epitaxial graphene in Figure 1d).[32,33] Moreover, the FFT diffraction pattern of C implies a crystal orientation similar to that of rGO, in agreement with the Raman spectroscopy results. The EDS images in Figure 1f of SiC/G@Pt clearly demonstrate that Pt catalysts on the surface of SiC/G are homogeneously distributed. In addition, the epitaxial graphene is located outside the SiC.

The activity and durability of the electrocatalyst for the ORR were determined using cyclic voltammetry (CV) and linear sweep voltammetry (LSV) with a rotating disk electrode (RDE) as well as fuel cell measurements. Table 1 compares the durability results of cycling tests, including the ECSA of the catalyst, mass activities, and half-wave potential. The CV curves of SiC/G@Pt and Pt/C were recorded for 5000 cycles, as shown in Figure 2, parts a and d, respectively. The initial ECSA (44.36 m^2/g_{pt}) of SiC/G@Pt was slightly less than that of Pt/C (47.62 m^2/g_{pt}), which might be explained by the lower electrical conductivity of the ceramic support as shown in Figure S3. On the other hand, the initial ECSA of SiC/G@Pt was significantly higher than that of the prepared SiC@Pt without rGO as shown in Figure S4. The results are indicated that the electrical conductivity of the catalysts facilitate charge transfer between the electrochemically active sites on the surface of the catalysts for improve the efficiency of the electrochemical reactions. Therefore, the higher electrical conductivity can enhance the overall electrocatalytic activity of the catalysts. In case of durable performance for supports, SiC/G support showed very durable performance, as evidenced by the ECSA loss of only 26.89% with SiC/G@Pt, which was much lower than that of Pt/C (36.88%) after 5000 cycles. This clearly indicates that the SiC/G support is significantly more durable than commercial Pt/C under the same accelerated electrochemical conditions.

LSV curves of SiC/G@Pt and Pt/C were also recorded to evaluate the catalytic ORR activity in an oxygen-saturated electrolyte, which can be determined from their half-wave potentials and limiting current values.[34,35] LSV curves of SiC/G@Pt and Pt/C were recorded with an RDE at 1600 rpm and a scan rate of 5 mV s^{-1}, as shown in Figure 2, parts b and e, respectively. Table 1 and Figure 2b,e show that the initial

https://doi.org/10.1021/acsaem.2c04073
ACS Appl. Energy Mater. 2023, 6, 4103−4110

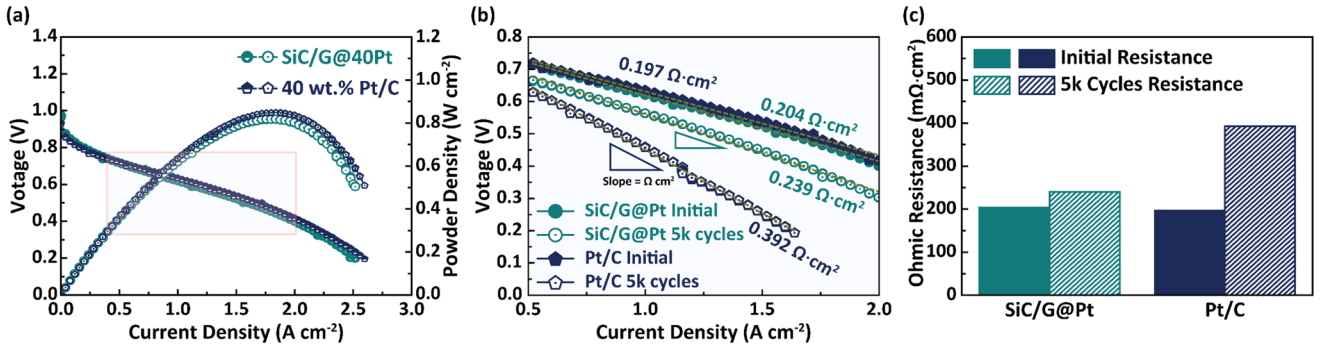

Figure 3. Electrochemical performance of SiC/G@Pt and Pt/C catalysts in PEMFCs. (a) $I-V$ polarization curves, (b) linear part of the $I-V$ curves in part a for determining the ohmic resistance, and (c) ohmic resistance before and after 5000 cycles.

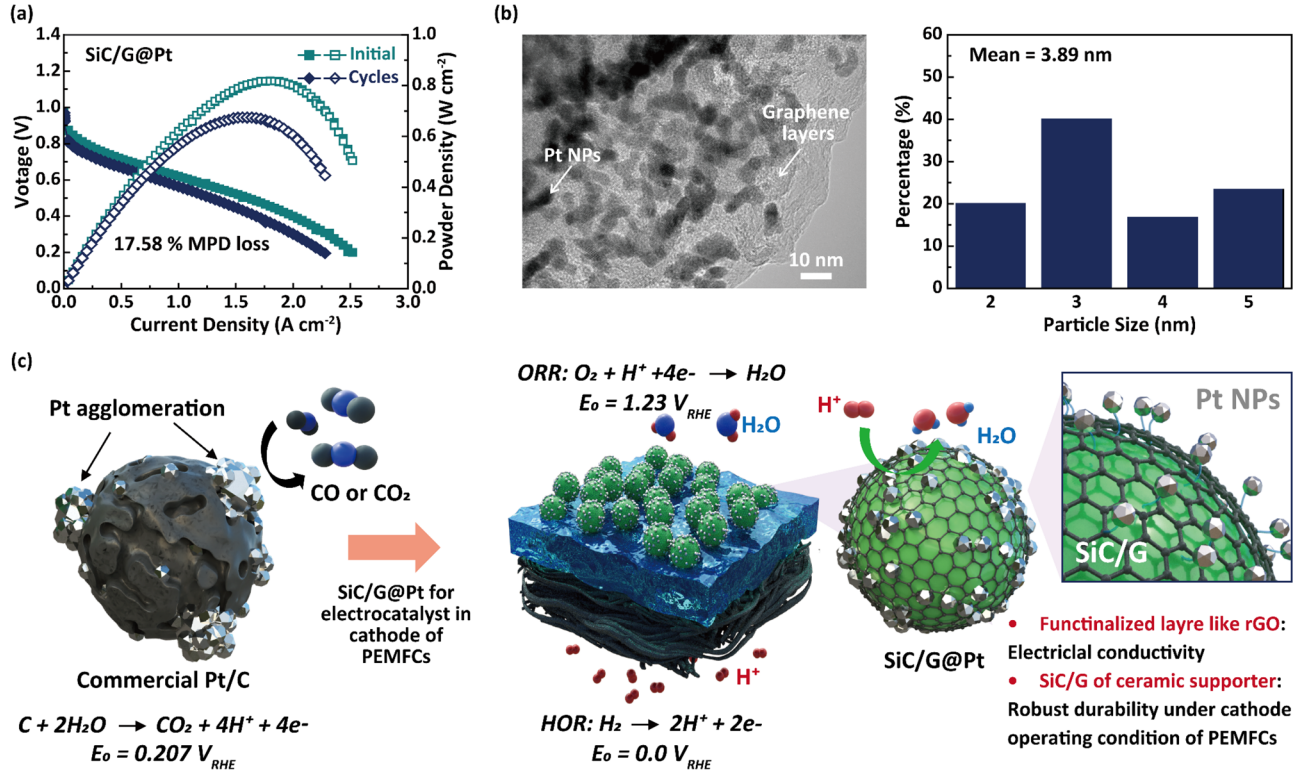

Figure 4. (a) $I-V$ polarization and power density curves and (b) TEM images of MEAs using SiC/G@Pt after ADT. (c) Schematic of the mechanism underlying the durability of SiC/G@Pt. A functionalized layer similar to rGO on the surface of SiC supplies the electrical conductivity. In addition, the SiC is maintained as robust support under the operating conditions of PEMFCs because of its good chemical and mechanical properties.

average mass activity of SiC/G@Pt (9.92 mA/g_{pt}) was less than that of Pt/C. However, the mass activity of Pt/C drastically decreased by 96.79% after 5000 cycles, whereas the mass activity of SiC/G@Pt decreased by only 15.93%. For this analysis, the mass activity was measured at 0.9 V vs the reversible hydrogen electrode (RHE). In addition, SiC/G@Pt shows a remarkable difference of 20 mV in the half-wave potential before and after 5000 cycles owing to carbon corrosion, which was smaller than that of Pt/C (140 mV). During degradation, several mechanisms commonly coincide with losses in the ECSA and mass activity, such as Pt agglomeration and carbon corrosion, as discussed above. As shown in Figure 2 and Table 1, the loss in ECSA of Pt/C was 36.88% after accelerated degradation testing (ADT), and its mass activity seriously decreased from the initial value of 11.20 mA mg_{Pt}^{-1} to 0.36 mA mg_{Pt}^{-1}, a decrease of 97%. In contrast, the ECSA loss of SiC/G@Pt was only 26.89%, and its initial mass activity was better maintained, decreasing by only 16% from 9.92 to 8.34 mA mg_{Pt}^{-1}. Although the initial electrocatalytic values (i.e., the ECSA and mass activity at 0.9 V) of Pt/C were slightly higher than those of SiC/G@Pt, their degradation rates were dramatically lower for SiC/G@Pt than those for Pt/C, implying that SiC/G@Pt is a promising robust support that avoids Pt agglomeration and carbon corrosion.

Figure 3a shows the current density−voltage ($I-V$) curves of PEMFCs using SiC/G@Pt and Pt/C electrocatalysts for the cathode. The open-circuit voltages (OCVs) of all species were recorded over 0.93 V at 70 °C, and no significant difference from the practical value was found because of the different support materials. As shown in Figure 3b, the ohmic resistance was calculated from the slope of the $I-V$ curve within the linear range from 0.5 to 2.0 A/cm^2; the value of SiC/G@Pt

https://doi.org/10.1021/acsaem.2c04073
ACS Appl. Energy Mater. 2023, 6, 4103−4110

Table 2. *I*−*V* Performance and Durability Results for the SiC/G@Pt and Pt/C Catalysts

sample	OCV (V)	MPD (W/cm^2)	MPD loss (%)	initial ohmic resistance ($\Omega \cdot cm^2$)	after ohmic resistance ($\Omega \cdot cm^2$)	Δ ohmic loss (mV) @ 0.5−2.0 V
SiC/G@Pt	0.975	0.82	17.58	0.204	0.239	11
Pt/C	0.933	0.85	63.26	0.197	0.392	75

(0.204 Ω cm^2) was similar to that of Pt/C (0.197 Ω cm^2) before cycling. This similarity might imply that SiC/G is sufficiently conductive to be used as catalyst support, comparable to the commercial carbon black in Pt/C. Therefore, we could infer that the poor electrical conductivity issues of ceramic support could be mitigated by the in situ assembly of graphene layers on the SiC surface. In any case, the maximum power densities (MPDs) of the cells using SiC/G and Pt/C were 0.82 and 0.85 W/cm^2, respectively. The values are observed to be higher than in comparison to those of previously reported metal oxide support-based catalysts (Table S2). Furthermore, the ohmic resistance of SiC/G@Pt increased by only 17.44% after 5000 cycles, which is a very small change that indicates the robustness of the SiC/G support. On the other hand, the resistance of Pt/C increased drastically from 0.197 to 0.392 Ω cm^2, which is an increase of 98% (Figure 3b,c).

Figure 4a shows *I*−*V* curves of the PEMFC system with SiC/G@Pt before and after ADT. The MPD after ADT decreased by approximately 17.58%, which is a significantly smaller loss than that of commercial Pt/C (63.26%), as shown in Figure S5a. The *I*−*V* performance and durability results are summarized in Table 2, which indicates the low carbon corrosion owing to the robustness and durability of SiC/G support. In addition, no serious Pt agglomeration occurs in the case of SiC/G@Pt, as demonstrated by the TEM image (Figure 4b) after ADT, as its appearance is similar to that in its initial state before ADT (Figure 1e). On the other hand, Pt agglomeration and detachment were evident in the TEM images of commercial Pt/C after ADT, as shown in Figure S5b,c. The mechanism underlying the durability of SiC/G@Pt is schematically illustrated in Figure 4c. Commonly, carbon-based materials are used as catalyst supports for PEMFCs because of their granular microporous layers and fibrous gas diffusion layers. These carbon-based supports are exposed to oxidizing conditions at the cathode. The electrocatalyst for the cathode is easily degraded in this environment, thereby worsening cell performance because of losses in the kinetics of the ORR and oxygen mass transport. One major degradation mechanism involving the electrocatalyst is oxidative corrosion of the porous carbon material used as the catalyst support during potential fluctuations generated by start-up/shutdown cycling. Specifically, water is the primary oxidant in the electrochemical carbon corrosion, and CO_2 is the ultimate product.[36,37]

$$C + 2H_2O \rightarrow CO_2 + 4H^+ + 4e^- \quad (3)$$

$$E^0 = 0.207\ V_{RHE} \quad (4)$$

The oxidation of the carbon support in the cathode decreases performance owing to the loss of active sites, the decreased electrical connectivity of the catalyst support structure within the electrode and the loss of Pt catalyst caused by Pt agglomeration (see Figure 4c: commercial Pt/C electrocatalysts). Although the kinetics of carbon oxidation are slow under the typical operating temperatures and potentials of PEMFCs, this reaction is catalyzed by Pt and occurs more rapidly in the presence of water formed during operation.[38] Thus, carbon corrosion is a major concern for the long-term durability of PEMFCs. In this study, the SiC/G@Pt electrocatalyst was applied at the cathode for PEMFCs (Figure 4c: SiC/G@Pt). A functionalized layer similar to rGO on the surface of SiC supplied the electrical conductivity to overcome the low electrical conductivity of the ceramic support and provided sites for the formation of Pt nanoparticles during the synthesis of the electrocatalyst. SiC was maintained as a robust support under the operating conditions of PEMFCs because of its good chemical and mechanical properties. Specifically, SiC/G@Pt was resistant to carbon corrosion, as shown in TEM results after ADT. Moreover, the Pt catalysts did not agglomerate and remained finely distributed on the support surface. Further, the minimized decreases in the ORR performance and electrocatalytic activity suggested that SiC/G@Pt degraded less than the commercial catalysts. Therefore, the SiC/G support shows excellent promise as an alternative to porous carbon supports for Pt catalysts thanks to its improved durability for PEMFC applications.

3. CONCLUSIONS

In conclusion, a Pt catalyst supported by nanographene-modified SiC (SiC/G@Pt) was successfully prepared using coffee grounds as the carbon source for the epitaxial growth of graphene. We proposed a possible mechanism underlying this carbon deposition: (i) gases formed during the thermal decomposition of coffee grounds and (ii) the surface layer for SiC also thermally decomposed because of the high processing temperature (above 1000 °C), thus supplying additional carbon. A functionalized layer similar to rGO on the surface of SiC effectively improved the surface electrocatalytic activity and interactions between Pt metal and the functionalized surface of the support. SiC/G@Pt showed excellent durability, delivering power densities of 0.42 and 0.39 W cm^{-2} at 0.7 V before and after ADT, respectively, a decrease of only 17%. The TEM results demonstrated that in contrast with commercial Pt/C, SiC/G@Pt showed no serious Pt agglomeration after ADT, whereas Pt evidently agglomerated and detached in commercial Pt/C after ADT. The excellent durability of SiC/G@Pt was attributed to the rGO-like functionalized layer on the surface of SiC, which also supplied electrical conductivity and sites for the formation of Pt nanoparticles to electrocatalyze the ORR. Therefore, the SiC/G support prepared from coffee grounds not only showed good prospects for replacing porous-carbon-based supports for PEMFC applications but also demonstrates the feasibility of using an organic waste product on the scale of mass commercialization.

■ ASSOCIATED CONTENT

Supporting Information

The Supporting Information is available free of charge at https://pubs.acs.org/doi/10.1021/acsaem.2c04073.

https://doi.org/10.1021/acsaem.2c04073
ACS Appl. Energy Mater. 2023, 6, 4103−4110

Experimental section and further material characterization including SEM images, EDS elemental mapping, XPS data, TEM data, apparent electrical conductivity, CV curves for calculation of ECSA, I−V polarization curves and recently reported metal oxide supported-based catalysts used in PEMFCs (PDF)

AUTHOR INFORMATION

Corresponding Authors

Tae Ho Shin − *Hydrogen Energy Materials Center, Korea Institute of Ceramic Engineering and Technology, Jinju 52851, Korea*; orcid.org/0000-0002-9001-7863; Email: ths@kicet.re.kr

Soon-Mok Choi − *School of Energy, Materials and Chemical Engineering, Korea University of Technology and Education, Cheonan 31253, Korea*; Email: smchoi@koreatech.ac.kr

Authors

Byeong Geun Kim − *Research Development Division, Gyeongbuk Institute of IT Convergence Industry Technology, Gyeongsan-si 38463, Korea*

Seokhee Lee − *Hydrogen Energy Materials Center, Korea Institute of Ceramic Engineering and Technology, Jinju 52851, Korea*

Yi kyeong Jung − *Hydrogen Energy Materials Center, Korea Institute of Ceramic Engineering and Technology, Jinju 52851, Korea*

Jin Uk Lee − *Hydrogen Energy Materials Center, Korea Institute of Ceramic Engineering and Technology, Jinju 52851, Korea*

Seoyoon Shin − *Hydrogen Energy Materials Center, Korea Institute of Ceramic Engineering and Technology, Jinju 52851, Korea*

Complete contact information is available at: https://pubs.acs.org/10.1021/acsaem.2c04073

Author Contributions

‖B.G.K. and S.L. contributed equally to this work.

Notes

The authors declare no competing financial interest.

ACKNOWLEDGMENTS

This work was supported by a National Research Foundation of Korea (NRF) grant funded by the Korea government (MSIT) (No. 2022R1A2C1092054) and the National R&D Program through the National Research Foundation of Korea (NRF) funded by the Ministry of Science and ICT (2020M3H4A3105824).

REFERENCES

(1) Debe, M. K. Electrocatalyst approaches and challenges for automotive fuel cells. *Nature* **2012**, *486* (7401), 43−51.

(2) Pollet, B. G.; Kocha, S. S.; Staffell, I. Current status of automotive fuel cells for sustainable transport. *Current Opinion in Electrochemistry* **2019**, *16*, 90−95.

(3) Namgung, Y.; Hong, J.; Kumar, A.; Lim, D.-K.; Song, S.-J. One step infiltration induced multi-cation oxide nanocatalyst for load proof SOFC application. *Appl. Catal. B: Environmental* **2020**, *267*, 118374.

(4) Zhao, L.; Zhu, J.; Zheng, Y.; Xiao, M.; Gao, R.; Zhang, Z.; Wen, G.; Dou, H.; Deng, Y. P.; Yu, A.; Wang, Z.; Chen, Z. Materials Engineering toward Durable Electrocatalysts for Proton Exchange Membrane Fuel Cells. *Adv. Energy Mater.* **2022**, *12* (2), 2102665.

(5) Zana, A.; Speder, J.; Roefzaad, M.; Altmann, L.; Bäumer, M.; Arenz, M. Probing Degradation by IL-TEM: The Influence of Stress Test Conditions on the Degradation Mechanism. *J. Electrochem. Soc.* **2013**, *160* (6), F608−F615.

(6) Reiser, C. A.; Bregoli, L.; Patterson, T. W.; Yi, J. S.; Yang, J. D.; Perry, M. L.; Jarvi, T. D. A Reverse-Current Decay Mechanism for Fuel Cells. *Electrochem. Solid-State Lett.* **2005**, *8* (6), A273.

(7) Marcu, A.; Toth, G.; Kundu, S.; Colmenares, L. C.; Behm, R. J. Ex situ testing method to characterize cathode catalysts degradation under simulated start-up/shut-down conditions − A contribution to polymer electrolyte membrane fuel cell benchmarking. *J. Power Sources* **2012**, *215*, 266−273.

(8) Bai, J.; Ke, S.; Song, J.; Wang, K.; Sun, C.; Zhang, J.; Dou, M. Surface Engineering of Carbon-Supported Platinum as a Route to Electrocatalysts with Superior Durability and Activity for PEMFC Cathodes. *ACS Appl. Mater. Interfaces* **2022**, *14* (4), 5287−5297.

(9) Hassen, D.; Shenashen, M. A.; El-Safty, S. A.; Selim, M. M.; Isago, H.; Elmarakbi, A.; El-Safty, A.; Yamaguchi, H. Nitrogen-doped carbon-embedded TiO2 nanofibers as promising oxygen reduction reaction electrocatalysts. *J. Power Sources* **2016**, *330*, 292−303.

(10) Sharma, S.; Pollet, B. G. Support materials for PEMFC and DMFC electrocatalysts—A review. *J. Power Sources* **2012**, *208*, 96−119.

(11) Huang, S.-Y.; Ganesan, P.; Park, S.; Popov, B. N. Development of a titanium dioxide-supported platinum catalyst with ultrahigh stability for polymer electrolyte membrane fuel cell applications. *J. Am. Chem. Soc.* **2009**, *131* (39), 13898−13899.

(12) Eckardt, M.; Gebauer, C.; Jusys, Z.; Wassner, M.; Hüsing, N.; Behm, R. J. Oxygen reduction reaction activity and long-term stability of platinum nanoparticles supported on titania and titania-carbon nanotube composites. *J. Power Sources* **2018**, *400*, 580−591.

(13) Lee, E.; Park, C.; Lee, D. W.; Lee, G.; Park, H.-Y.; Jang, J. H.; Kim, H.-J.; Sung, Y.-E.; Tak, Y.; Yoo, S. J. Tunable Synthesis of N,C-Codoped Ti^{3+}-Enriched Titanium Oxide Support for Highly Durable PEMFC Cathode. *ACS Catal.* **2020**, *10* (20), 12080−12090.

(14) Pujol, D.; Liu, C.; Gominho, J.; Olivella, M. À.; Fiol, N.; Villaescusa, I.; Pereira, H. The chemical composition of exhausted coffee waste. *Industrial Crops and Products* **2013**, *50*, 423−429.

(15) Bronikowski, M. J.; Willis, P. A.; Colbert, D. T.; Smith, K.; Smalley, R. E. Gas-phase production of carbon single-walled nanotubes from carbon monoxide via the HiPco process: A parametric study. *Journal of Vacuum Science & Technology A: Vacuum, Surfaces, and Films* **2001**, *19* (4), 1800−1805.

(16) Nikolaev, P.; Bronikowski, M. J.; Bradley, R. K.; Rohmund, F.; Colbert, D. T.; Smith, K.; Smalley, R. E. Gas-phase catalytic growth of single-walled carbon nanotubes from carbon monoxide. *Chemical physics letters* **1999**, *313* (1−2), 91−97.

(17) Kim, C.-D.; Min, B.-K.; Jung, W.-S. Preparation of graphene sheets by the reduction of carbon monoxide. *Carbon* **2009**, *47* (6), 1610−1612.

(18) Chen, M.; Chen, C.-M.; Chen, C.-F. Growth of carbon nanotubes by microwave plasma chemical vapor deposition using CH4 and CO2 gas mixture. *Thin Solid Films* **2002**, *420*, 230−234.

(19) Wang, X.; You, H.; Liu, F.; Li, M.; Wan, L.; Li, S.; Li, Q.; Xu, Y.; Tian, R.; Yu, Z.; et al. Large-scale synthesis of few-layered graphene using CVD. *Chem. Vap. Deposition* **2009**, *15* (1−3), 53−56.

(20) De Arco, L. G.; Zhang, Y.; Kumar, A.; Zhou, C. Synthesis, transfer, and devices of single-and few-layer graphene by chemical vapor deposition. *IEEE Transactions on Nanotechnology* **2009**, *8* (2), 135−138.

(21) Norimatsu, W.; Kusunoki, M. Growth of graphene from SiC {0001} surfaces and its mechanisms. *Semicond. Sci. Technol.* **2014**, *29* (6), 064009.

(22) Riedl, C.; Coletti, C.; Iwasaki, T.; Zakharov, A.; Starke, U. Quasi-free-standing epitaxial graphene on SiC obtained by hydrogen intercalation. *Physical review letters* **2009**, *103* (24), 246804.

(23) Kim, B. G.; Nam, D.-H.; Jeong, S.-M.; Lee, M.-H.; Seo, W.-S.; Choi, S.-M. One-step growth of multilayer-graphene hollow nano-

spheres via the self-elimination of SiC nuclei templates. *Sci. Rep.* **2017**, *7* (1), 1−8.
(24) Jabbar, A.; Yasin, G.; Khan, W. Q.; Anwar, M. Y.; Korai, R. M.; Nizam, M. N.; Muhyodin, G. Electrochemical deposition of nickel graphene composite coatings: effect of deposition temperature on its surface morphology and corrosion resistance. *RSC Adv.* **2017**, *7* (49), 31100−31109.
(25) Stankovich, S.; Dikin, D. A.; Piner, R. D.; Kohlhaas, K. A.; Kleinhammes, A.; Jia, Y.; Wu, Y.; Nguyen, S. T.; Ruoff, R. S. Synthesis of graphene-based nanosheets via chemical reduction of exfoliated graphite oxide. *carbon* **2007**, *45* (7), 1558−1565.
(26) Sivalingam, M. M.; Balasubramanian, K. Influence of the concentration of reducing agent on gold nanoparticles decorated reduced graphene oxide and its ammonia sensing performance. *Appl. Phys. A: Mater. Sci. Process.* **2017**, *123* (4), 1−9.
(27) Palaniselvam, T.; Aiyappa, H. B.; Kurungot, S. An efficient oxygen reduction electrocatalyst from graphene by simultaneously generating pores and nitrogen doped active sites. *J. Mater. Chem.* **2012**, *22* (45), 23799−23805.
(28) Kim, S.-G.; Park, O.-K.; Lee, J. H.; Ku, B.-C. Layer-by-layer assembled graphene oxide films and barrier properties of thermally reduced graphene oxide membranes. *Carbon letters* **2013**, *14* (4), 247−250.
(29) Akalework, N. G.; Pan, C. J.; Su, W. N.; Rick, J.; Tsai, M. C.; Lee, J. F.; Lin, J.-M.; Tsai, L.-D.; Hwang, B. J. Ultrathin TiO_2-coated MWCNTs with excellent conductivity and SMSI nature as Pt catalyst support for oxygen reduction reaction in PEMFCs. *J. Mater. Chem.* **2012**, *22* (39), 20977−20985.
(30) Alipour Moghadam Esfahani, R.; Easton, E. B. Exceptionally durable Pt/TOMS catalysts for fuel cells. *Appl. Catal. B: Environmental* **2020**, *268*, 118743.
(31) Sinniah, J. D.; Wong, W. Y.; Loh, K. S.; Yunus, R. M.; Timmiati, S. N. Perspectives on carbon-alternative materials as Pt catalyst supports for a durable oxygen reduction reaction in proton exchange membrane fuel cells. *J. Power Sources* **2022**, *534*, 231422.
(32) Shalaby, A.; Nihtianova, D.; Markov, P.; Staneva, A. D.; Iordanova, R. S.; Dimitriev, Y. B. Structural analysis of reduced graphene oxide by transmission electron microscopy. *Bulgarian Chemical Communications* **2015**, *47* (1), 291−295.
(33) Riaz, A.; Saeed, M.; Munir, M.; Intisar, A.; Haider, S.; Tariq, S.; Hussain, N.; Kousar, R.; Bilal, M. Development of reduced graphene oxide-supported novel hybrid nanomaterials (Bi_2WO_6@rGO and $CuWO_4$@rGO) for green and efficient oxidative desulfurization of model fuel oil for environmental depollution. *Environmental Research* **2022**, *212*, 113160.
(34) Kabiraz, M. K.; Ruqia, B.; Kim, J.; Kim, H.; Kim, H. J.; Hong, Y.; Kim, M. J.; Kim, Y. K.; Kim, C.; Lee, W.-J.; et al. Understanding the Grain Boundary Behavior of Bimetallic Platinum−Cobalt Alloy Nanowires toward Oxygen Electro-Reduction. *ACS Catal.* **2022**, *12* (6), 3516−3523.
(35) Kim, J.; Kim, H. J.; Ruqia, B.; Kim, M. J.; Jang, Y. J.; Jo, T. H.; Baik, H.; Oh, H. S.; Chung, H. S.; Baek, K. Crystal phase transition creates a highly active and stable RuCx nanosurface for hydrogen evolution reaction in alkaline media. *Adv. Mater.* **2021**, *33* (48), 2105248.
(36) Wang, X. X.; Swihart, M. T.; Wu, G. Achievements, challenges and perspectives on cathode catalysts in proton exchange membrane fuel cells for transportation. *Nature Catalysis* **2019**, *2* (7), 578−589.
(37) Cullen, D. A.; Neyerlin, K.; Ahluwalia, R. K.; Mukundan, R.; More, K. L.; Borup, R. L.; Weber, A. Z.; Myers, D. J.; Kusoglu, A. New roads and challenges for fuel cells in heavy-duty transportation. *N.ature energy* **2021**, *6* (5), 462−474.
(38) Chang, Q.; Hong, Y.; Lee, H. J.; Lee, J. H.; Ologunagba, D.; Liang, Z.; Kim, J.; Kim, M. J.; Hong, J. W.; Song, L.; et al. Achieving complete electrooxidation of ethanol by single atomic Rh decoration of Pt nanocubes. *Proc. Natl. Acad. Sci. U. S. A.* **2022**, *119* (11), e2112109119.

https://doi.org/10.1021/acsaem.2c04073
ACS Appl. Energy Mater. 2023, 6, 4103−4110